



Cite this: *RSC Adv.*, 2017, 7, 32488

# Visible light sensitization of TiO<sub>2</sub> nanoparticles by a dietary pigment, curcumin, for environmental photochemical transformations†

Jonghun Lim, Alok D. Bokare ‡ and Wonyong Choi \*

The use of curcumin, an active ingredient of turmeric powder (a dye component in curry), as a TiO<sub>2</sub> photo-sensitizer was investigated in terms of the photochemical and photoelectrochemical (PEC) properties. Owing to its strong visible light absorption and strong surface complexation, the curcumin-sensitized TiO<sub>2</sub> composite exhibited notable activities for the photochemical degradation of organic compounds, the reduction of chromate (Cr(vi)), and the generation of OH radicals and H<sub>2</sub>O<sub>2</sub> through the reduction of O<sub>2</sub> under visible light ( $\lambda > 420$  nm). Various spectroscopic methods confirmed the anchoring of curcumin on TiO<sub>2</sub> and the photochemical and PEC properties of curcumin/TiO<sub>2</sub> were compared with those of TiO<sub>2</sub> sensitized by a ruthenium complex (RuL<sub>3</sub>) that has been frequently employed as a visible light sensitizer. Curcumin/TiO<sub>2</sub> exhibited consistently higher photochemical and PEC activities than RuL<sub>3</sub>/TiO<sub>2</sub> over a wide pH range in an aquatic environment. These results confirm the practical viability of using a natural food dye, curcumin, as an efficient, eco-friendly, and cheap photo-sensitizer of TiO<sub>2</sub> for solar environmental applications. However, it should be noted that curcumin on TiO<sub>2</sub> like other dye sensitizers is degraded as a result of the sensitizing reactions in water and should be considered as a sensitizing reagent, not a photocatalyst.

Received 10th May 2017  
Accepted 12th June 2017

DOI: 10.1039/c7ra05276f

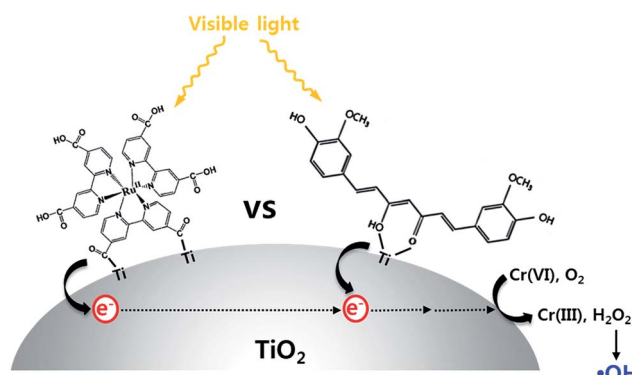
rsc.li/rsc-advances

## Introduction

Titanium dioxide (TiO<sub>2</sub>) is one of the most popular photo-catalysts, but it suffers from a lack of visible light absorption because of a large bandgap ( $\sim 3$  eV).<sup>1–3</sup> Various strategies have been attempted to increase the visible light absorption of wide bandgap semiconductors such as doping with metal or non-metal elements,<sup>4–8</sup> surface deposition of noble metals for plasmon effects,<sup>9–11</sup> and coupling with smaller bandgap semiconductors,<sup>12–14</sup> quantum dots<sup>15,16</sup> and dyes.<sup>17–19</sup> Among them, dye sensitization has been successfully demonstrated for many applications such as photocatalytic hydrogen production<sup>20,21</sup> and dye-sensitized solar cells.<sup>22</sup> In particular, ruthenium-based dyes have been widely used because of their high visible light absorption efficiency and stability in acidic aquatic environments.<sup>23,24</sup> However, it is not economical and environmentally benign, because ruthenium is not only expensive but also hazardous. Therefore, many researchers have synthesized organic dye sensitizers to replace the Ru-based dyes. Although various organic dyes have been successfully synthesized and

tested for their photosensitizing effects,<sup>18,25,26</sup> the complex synthetic procedures and long processing time of dye preparation are serious drawbacks.

Curcumin, a natural ingredient (1.8–2.0%) in commercial turmeric powder, is a yellow pigment that is widely used as food additive and supplement. The chemical structure of curcumin consists of two phenolic groups which are connected by two  $\alpha,\beta$ -unsaturated carbonyl groups exhibiting keto–enol tautomerism (see Scheme 1 for the molecular structure). It has been used in various research fields of physics, chemistry, biology and



**Scheme 1** Schematic illustration of the structure of curcumin-complexed TiO<sub>2</sub> vs. RuL<sub>3</sub>-complexed TiO<sub>2</sub> (compared as a control).

Division of Environmental Science and Engineering, Pohang University of Science and Technology (POSTECH), Pohang 37673, Korea. E-mail: wchoi@postech.edu; Fax: +82-54-279-8299

† Electronic supplementary information (ESI) available. See DOI: 10.1039/c7ra05276f

‡ In memory of Dr. Alok D. Bokare.



medicine because of its non-toxicity, biocompatibility, and natural occurrence.<sup>27–32</sup> The photo-physical and photo-chemical properties of curcumin have been applied for medicinal applications such as skin protection<sup>27</sup> and energy applications like dye-sensitized solar cells.<sup>33</sup> In the case of dye-sensitized solar cell using curcumin dye, the conversion efficiency (about 1%) was much lower than that obtained using Ru-based dye.<sup>33</sup> However, we note that the environmentally benign nature of curcumin makes it an ideal dye sensitizer for environmental photochemical conversions that work under visible light, which has not been investigated yet. Owing to its eco-friendly properties (non-toxic nature, biocompatibility and natural occurrence), curcumin offers a much better practical alternative to any organometallic dyes including Ru-based complexes.

In this work, we investigated the use of curcumin-sensitized TiO<sub>2</sub> for eco-friendly photochemical applications. The curcumin sensitizer was successfully adsorbed on the TiO<sub>2</sub> surface in aqueous suspension and the dye-TiO<sub>2</sub> composite was characterized by various spectroscopic and electrochemical analyses. Under visible light ( $\lambda > 420$  nm) irradiation, the photochemical and photoelectrochemical (PEC) properties of curcumin/TiO<sub>2</sub> were compared with a traditional ruthenium-dye/TiO<sub>2</sub> system. The curcumin/TiO<sub>2</sub> system not only showed enhanced photochemical and PEC properties, but also exhibited superior stability in water over a wide pH range.

## Experimental

### Materials and chemicals

TiO<sub>2</sub> powder (P25), a mixture of anatase and rutile (8 : 2) with a BET surface area of  $\sim 50$  m<sup>2</sup> g<sup>-1</sup> and primary particle size of 20–30 nm, was used as a base catalyst material. Commercial curcumin powder (Acros Organics) was employed as the sensitizer. Ru<sup>II</sup>(4,4-bipyridine-dicarboxylic acid) (RuL<sub>3</sub>) was synthesized according to our previous method<sup>24</sup> and compared as a control dye throughout the study. The chemicals used in this work were Na<sub>2</sub>Cr<sub>2</sub>O<sub>7</sub> (Cr(vi), Aldrich), dichloroacetate (DCA, Aldrich), tetramethylammonium chloride (TMA, Acros), *tert*-butanol (*t*-BuOH, Aldrich), coumarin (Sigma), ethanol (94.5%, SAMCHUN), 5,5-dimethyl-1-pyrroline-*N*-oxide (DMPO, Sigma-Aldrich), sodium perchlorate (98%, Aldrich), and polyethylene glycol (PEG, Aldrich, molecular weight 20 kDa). All reagents were used as received.

### Sample preparation

The adsorption of dye (curcumin or RuL<sub>3</sub>) on TiO<sub>2</sub> surface was done in acidic aqueous suspension. TiO<sub>2</sub> powder (0.1 g) was dispersed in 10 mL aqueous dye solution (RuL<sub>3</sub> and curcumin was dissolved in deionized water and ethanol, respectively) at pH 3. Several concentrations (25, 50, 75, and 100  $\mu$ M) of curcumin were tested and the optimal concentration was determined at 50  $\mu$ M. The solution was stirred for 3 h, and then the dye/TiO<sub>2</sub> sample was collected by filtering. After drying in an oven (85 °C), orange colored powder of dye/TiO<sub>2</sub> was obtained.

### Characterization of photocatalysts

Diffuse reflectance UV/visible absorption spectra were obtained using a spectrophotometer (Shimadzu UV-2401 PC) with an integrating sphere attachment and BaSO<sub>4</sub> was used as the reference. The surface chemical composition of curcumin/TiO<sub>2</sub> was determined by X-ray photoelectron spectroscopy (XPS) (Kratos XSAM 800 pci) using the Mg K $\alpha$  line (1253.6 eV) as the excitation source. The binding energies of all peaks were referenced to the C 1s line (284.6 eV). The presence and distribution of C and Ti elements in the curcumin/TiO<sub>2</sub> particles were confirmed using a high-resolution transmission electron microscope (HR-TEM, JEM-2100F microscope with Cs-correction). FT-IR spectra were measured using thin sample pellets (referenced against a KBr pellet) on a Bomem DA8 FT-IR spectrophotometer. The photoluminescence emission spectra of curcumin were measured using a spectrofluorometer (HORIBA, Fluoromax 4C-TCSPC).

### Photochemical activity test

The visible light activities of TiO<sub>2</sub> sensitized by curcumin and Ru-dye were tested for the reduction of chromate (Cr(vi)) and the degradation of dichloroacetate (DCA) and tetramethylammonium (TMA). The catalyst sample was dispersed in distilled water (0.5 g L<sup>-1</sup>) and an aliquot of the substrate stock solution was subsequently added to the suspension to give a desired substrate concentration. The initial pH of the suspension was adjusted to 3 with HClO<sub>4</sub> standard solution for the reduction of Cr(vi) and the degradation of DCA and TMA. The light source employed was a 300 W Xe arc lamp (Oriol). Light from the source passed through a 10 cm IR water filter and a UV cutoff filter transmitting ( $\lambda > 420$  nm for visible light irradiation) and then was focused onto a 30 mL Pyrex reactor with a quartz window.

Sample aliquots were withdrawn from the reactor at a given time interval during the irradiation and filtered through a 0.45  $\mu$ m PTFE syringe filter (Millipore) to remove the powder samples prior to analysis. The concentrations of ionic substrates and products were quantitatively analyzed using an ion chromatograph (IC, Dionex DX-120) that was equipped with a conductivity detector and Dionex Ionpac CS-14 (4 mm  $\times$  250 mm) for cation (TMA) analysis or AS-14 (4 mm  $\times$  250 mm) column for anion (DCA and Cl<sup>-</sup>) analysis. For the cation analysis, 10 mM methanesulfonic acid was used and 3.5 mM Na<sub>2</sub>CO<sub>3</sub>/1 mM NaHCO<sub>3</sub> was used for the anion analysis. The concentration of Cr(vi) was analyzed using a colorimetric method employing 1,5-diphenylcarbazide (DPC) reagent.<sup>34</sup> The concentration of photogenerated H<sub>2</sub>O<sub>2</sub> was determined by a colorimetric DPD method.<sup>35</sup> The absorption change was monitored at 540 nm ( $\epsilon = 6850$  M<sup>-1</sup> cm<sup>-1</sup>)<sup>36</sup> for Cr(vi) and at 551 nm ( $\epsilon = 2 \times 10^4$  M<sup>-1</sup> cm<sup>-1</sup>)<sup>35</sup> for H<sub>2</sub>O<sub>2</sub> using a UV/Vis spectrophotometer (Agilent 8453).

The production of OH radicals was indirectly monitored using coumarin as a chemical trap, which is oxidatively converted into 7-hydroxycoumarin (7-HC) through the reaction with  $\cdot$ OH (coumarin +  $\cdot$ OH  $\rightarrow$  7-HC).<sup>37</sup> The hydroxylated product was quantified by measuring the fluorescence emission intensity at



460 nm under the excitation at 332 nm. For electron paramagnetic resonance (EPR) analysis, 5,5-dimethyl-1-pyrroline-*N*-oxide (DMPO) was used as a spin-trapping agent for OH radical. The EPR spectra of DMPO-OH were monitored using a JES-TE 300 spectrometer (JEOL, Japan). EPR was measured with the conditions of microwave power of 3 mW, microwave frequency of 9.42 GHz, center field 338.25 mT, modulation width of 0.2 mT, and modulation frequency of 100 kHz.

### Photoelectrochemical (PEC) measurements

All PEC measurements were carried out in a conventional three-electrode cell using a computer-controlled potentiostat (Gamry, Reference 600). The PEC reactor was stirred and bubbled with nitrogen. The catalyst-coated photoanode, a Ag/AgCl (3.0 M NaCl) electrode and a Pt wire (when electrochemical impedance spectrum (EIS) was measured) or a graphite rod (when photocurrent was measured) were used as a working, a reference and a counter electrode, respectively. The working electrode was fabricated using Carbowax as a binder. TiO<sub>2</sub> powder was added in the solution of mixture of poly(ethylene glycol) (PEG, Aldrich, molecular weight: 20 kDa) and distilled water (50 wt%) and coated on a FTO plate using the doctor-blade method with tracks of two layers of Scotch tape. The TiO<sub>2</sub>-coated electrode was calcined at 450 °C for 1 h, cooled to room temperature and then immersed into an acidic solution (pH 3) of dye (curcumin and RuL<sub>3</sub> were dissolved in ethanol and distilled water, respectively) over 12 h to prepare the dye-adsorbed TiO<sub>2</sub>/FTO electrode. The photoanode was immersed in NaClO<sub>4</sub> solution and the potential bias was set at +0.6 V (vs. Ag/AgCl) during PEC measurements.

## Results and discussion

### Characterization of photocatalysts

The spectroscopic and electrochemical parameters of curcumin and Ru-dye are compared in Table 1. Because curcumin has a far more negative LUMO (lowest unoccupied molecular orbital) level than Ru-dye, the thermodynamic driving force for the electron transfer to the semiconductor conduction band (CB) should be higher compared to that of Ru-dye/TiO<sub>2</sub>. The optical absorption properties of the curcumin/TiO<sub>2</sub> samples with various loadings of curcumin are represented by their diffuse reflectance spectra (Fig. 1). Bare TiO<sub>2</sub> cannot absorb visible light due to its large bandgap (~3.0 eV), and the visible light absorption of curcumin/TiO<sub>2</sub> increased with increasing curcumin concentration in the curcumin absorption spectral

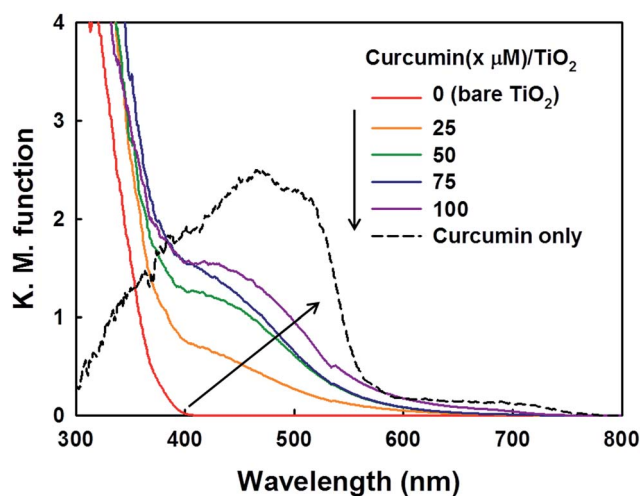


Fig. 1 Diffuse reflectance UV/visible spectra of bare TiO<sub>2</sub>, curcumin, and curcumin/TiO<sub>2</sub>.

region, which confirms the successful loading of curcumin on the surface of TiO<sub>2</sub> nanoparticles.

To confirm the adsorption of curcumin on the TiO<sub>2</sub> surface, FT-IR spectra of curcumin/TiO<sub>2</sub> was compared with that of bare TiO<sub>2</sub> and curcumin powder. As shown in Fig. S1a,† the curcumin/TiO<sub>2</sub> sample exhibits two distinct peaks at 1691 cm<sup>-1</sup> and 1507 cm<sup>-1</sup>, which correspond to the C=O and C=C functional groups of curcumin, respectively.<sup>38</sup> This also confirms that curcumin is adsorbed on the TiO<sub>2</sub> surface. The C=O peak was slightly shifted to a higher wavenumber, which indicates that the β-diketone group in curcumin forms a chelate complex on the TiO<sub>2</sub> surface.<sup>39</sup> The adsorption of curcumin on TiO<sub>2</sub> was also corroborated through C 1s and O 1s XPS analysis (Fig. S1b and c†). The peak intensities corresponding to C=O (at 287.7 eV for C 1s and at 531.7 eV for O 1s), C-O (at 286.5 eV for C 1s and 533.2 eV for O 1s), and C-C (at 284.9 eV for C 1s)<sup>40,41</sup> considerably increased compared to bare TiO<sub>2</sub>. Furthermore, the peaks at 288.6 eV for C 1s and 533.2 eV for O 1s corresponding to C-OH<sup>6</sup> newly appeared in curcumin/TiO<sub>2</sub>. Lastly, the presence of organic carbons (curcumin) on the TiO<sub>2</sub> surface was confirmed by electron energy loss spectroscopy (EELS) mapping (Fig. S2†). The Ti species were clearly identified in both bare TiO<sub>2</sub> and curcumin/TiO<sub>2</sub> samples, whereas the C species was only observed in the curcumin/TiO<sub>2</sub> sample. All these spectroscopic and microscopic analyses confirm that curcumin is adsorbed on the TiO<sub>2</sub> surface through complexation as depicted in Scheme 1.

Table 1 Spectroscopic and electrochemical properties of curcumin and RuL<sub>3</sub>

Dye	$\lambda_{\text{max}}/\text{nm}$	$\epsilon_{\text{max}}/\text{M}^{-1} \text{ cm}^{-1}$	$\Delta E^b/\text{V}$	$E^0(\text{dye}/\text{dye}^{*+})/\text{V}_{\text{NHE}}$	$E^0(\text{dye}^*/\text{dye}^{*+})/\text{V}_{\text{NHE}}$
Cur	424	48 000 <sup>a</sup>	2.64	0.55 <sup>d</sup>	-2.09 <sup>d</sup>
RuL <sub>3</sub> <sup>c</sup>	465	21 200	2.20	1.39	-0.81

<sup>a</sup> Ref. 51. <sup>b</sup> HOMO-LUMO gap. <sup>c</sup> Ref. 24. <sup>d</sup> Ref. 52.



### Photochemical and photoelectrochemical activity tests under visible light

The photochemical activities of as-prepared samples were evaluated for the reduction of Cr(vi) to Cr(III) (less toxic form) and the degradation of DCA and TMA under visible light ( $\lambda > 420$  nm). First of all, the photochemical reduction of Cr(vi) with curcumin/TiO<sub>2</sub> was compared with that of bare TiO<sub>2</sub> and RuL<sub>3</sub>/TiO<sub>2</sub> in the presence of ethanol as a hole scavenger. Although the adsorption of curcumin on TiO<sub>2</sub> surface steadily increased with increasing the concentration of curcumin up to 100  $\mu$ M, the photochemical activity for Cr(vi) reduction was maximized at the curcumin concentration of 50  $\mu$ M (Fig. 2a). Therefore, the curcumin concentration was fixed at 50  $\mu$ M for all visible light activity tests. The control catalyst of RuL<sub>3</sub>/TiO<sub>2</sub> was also prepared using the sensitizer concentration of 50  $\mu$ M. Fig. 2b shows the time profiles of photochemical reduction of Cr(vi) in the visible light illuminated catalyst suspension. For the control experiments, the reduction of Cr(vi) was tested with curcumin only and bare TiO<sub>2</sub> under visible light and curcumin/TiO<sub>2</sub> in the dark condition. The visible light-sensitized reduction of Cr(vi) by curcumin only and the adsorption of Cr(vi) on curcumin/TiO<sub>2</sub> surface were negligible. The activity of bare TiO<sub>2</sub> was very low because of the lack of visible light absorption. When dye (curcumin or Ru-dye) was adsorbed on TiO<sub>2</sub> surface, the activity was markedly enhanced. This result is ascribed to fact that excitation of dye under visible light induced the transfer of photo-generated electrons to CB of TiO<sub>2</sub> and further reaction with Cr(vi). Since curcumin has a higher absorption coefficient of visible light and a more negative LUMO level than RuL<sub>3</sub> (Table 1), the electron transfer from dye LUMO to TiO<sub>2</sub> CB should be more efficient in curcumin/TiO<sub>2</sub> than RuL<sub>3</sub>/TiO<sub>2</sub>. As a result, the photochemical reduction of Cr(vi) is far more efficient with curcumin/TiO<sub>2</sub> than RuL<sub>3</sub>/TiO<sub>2</sub>. The wavelength-dependent activities for Cr(vi) reduction (Fig. 2c) are consistent with the dye absorption spectral profiles, which confirms the dye sensitization mechanism. The photoluminescence (PL) intensity of curcumin was completely quenched in the presence of TiO<sub>2</sub> (Fig. S3†), which further supports the dye sensitization mechanism on curcumin/TiO<sub>2</sub> under visible light.

Fig. 3 compares the time profiles of the photochemical degradation of DCA (with TOC removal) and TMA under visible light irradiation with bare TiO<sub>2</sub>, RuL<sub>3</sub>/TiO<sub>2</sub>, and curcumin/TiO<sub>2</sub>. For all cases, curcumin/TiO<sub>2</sub> exhibited the higher visible light activity than others, which is consistent with the photochemical reduction of Cr(vi) (see Fig. 2). This demonstrates that the curcumin/TiO<sub>2</sub> is efficient in the photooxidative conversion as well as the photoreductive conversion. The photochemical degradation of DCA and TMA with curcumin/TiO<sub>2</sub> was completely inhibited in the presence of excess *t*-BuOH ( $\cdot$ OH scavenger), which implies that OH radicals are involved as a major oxidant in this visible light-sensitized system. TMA is a very recalcitrant compound that can be degraded by OH radicals only,<sup>42,43</sup> and its successful degradation under visible light is a clear indication of OH radical generation through the sensitization process. Since the curcumin HOMO level (0.55 V<sub>NHE</sub>) is not energetic enough to generate  $\cdot$ OH ( $E^0(\cdot\text{OH}/\text{H}_2\text{O}) = 2.77$  V<sub>NHE</sub>), the

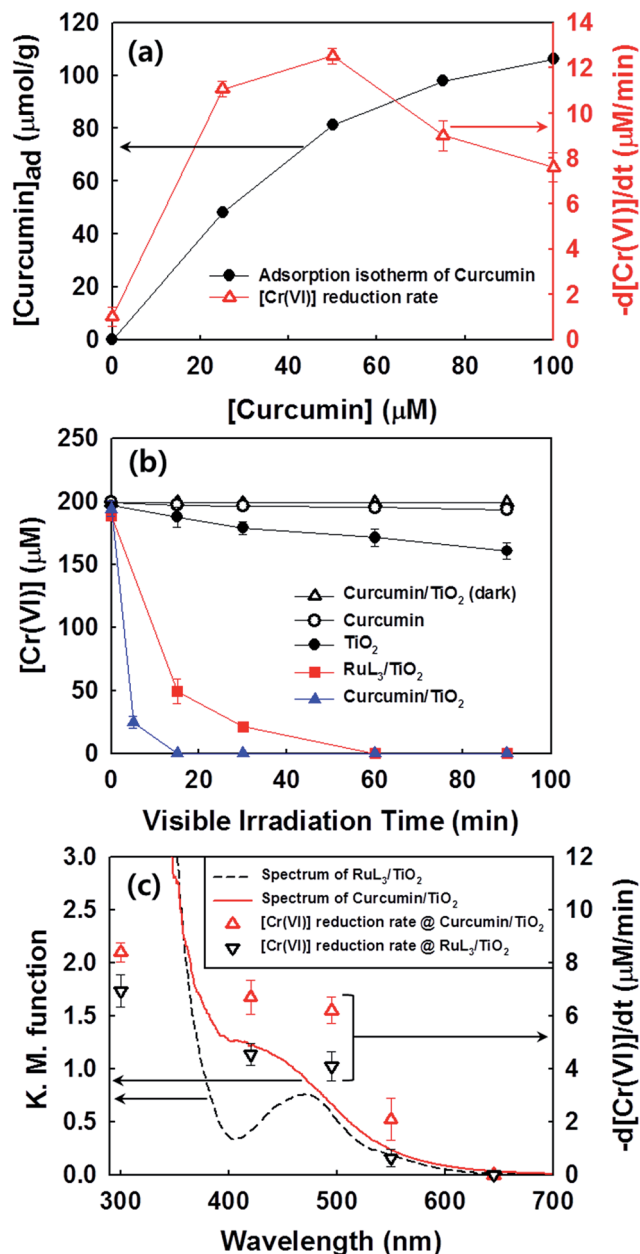


Fig. 2 (a) Visible light-sensitized reduction of Cr(vi) on TiO<sub>2</sub> as a function of the curcumin concentration and the adsorption isotherm of curcumin in the aqueous suspension of TiO<sub>2</sub>. (b) Time profiles of visible light-induced removal of Cr(vi) in catalyst suspensions, and (c) the removal rates of Cr(vi) on dye/TiO<sub>2</sub> as a function of the irradiation wavelength. The diffuse reflectance spectra of curcumin/TiO<sub>2</sub> and RuL<sub>3</sub>/TiO<sub>2</sub> are compared. The wavelength in the x-axis refers to the cutoff  $\lambda$  of the longpass filter ( $\lambda_{\text{irrad}} > \text{cutoff } \lambda$ ). The experimental conditions were [catalyst] = 0.5 g L<sup>-1</sup>, [Cr(vi)]<sub>0</sub> = 200  $\mu$ M, [EtOH]<sub>0</sub> = 10 mM, pH<sub>0</sub> = 3.0,  $\lambda > 420$  nm (for a and b), air-equilibrated for 30 min prior to irradiation.

generation of  $\cdot$ OH in the sensitization system should be mediated by the reductive conversion of O<sub>2</sub> (O<sub>2</sub>  $\rightarrow$  HO<sub>2</sub> $\cdot$   $\rightarrow$  H<sub>2</sub>O<sub>2</sub>  $\rightarrow$   $\cdot$ OH).<sup>44</sup> To confirm the generation of  $\cdot$ OH through the reduction of O<sub>2</sub>, the production of intermediate H<sub>2</sub>O<sub>2</sub> was confirmed (see Fig. 4a). When the suspension of curcumin/TiO<sub>2</sub> was purged with argon gas, H<sub>2</sub>O<sub>2</sub> was not produced at all because of the

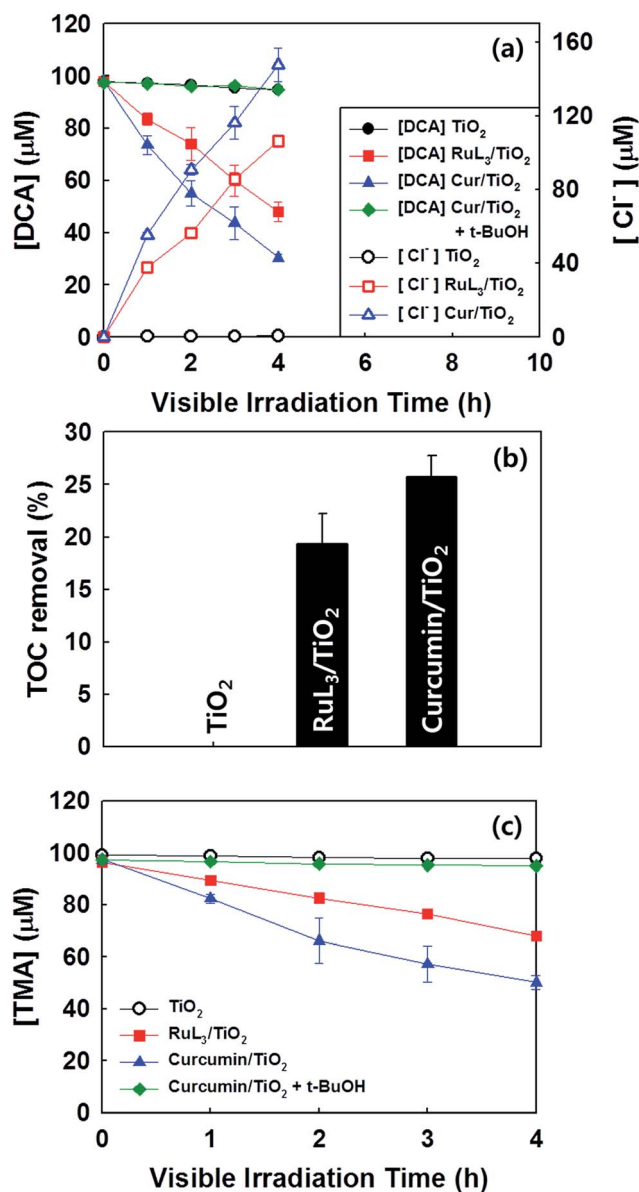


Fig. 3 (a) Visible light-sensitized degradation of DCA with the accompanying production of chloride, (b) TOC removal efficiencies after 4 h photodegradation of DCA, (c) visible light-sensitized degradation of TMA with bare TiO<sub>2</sub>, RuL<sub>3</sub>/TiO<sub>2</sub>, and curcumin/TiO<sub>2</sub>. The experimental conditions were [catalyst] = 0.5 g L<sup>-1</sup>, [DCA]<sub>0</sub> = [TMA]<sub>0</sub> = 100 μM, [t-BuOH] = 100 mM (for a and c), pH<sub>0</sub> = 3.0, λ > 420 nm, air-equilibrated for 30 min prior to irradiation.

absence of O<sub>2</sub>, which further confirms that H<sub>2</sub>O<sub>2</sub> is generated *via* O<sub>2</sub> reduction. In addition, a chemical trapping of <sup>•</sup>OH was tested as an indirect method of confirming the generation of <sup>•</sup>OH: the reaction of coumarin with <sup>•</sup>OH, which induces the formation of coumarin-OH adduct (<sup>•</sup>OH + coumarin → 7-hydroxycoumarin (7-HC)), was monitored and quantitatively analyzed (see Fig. 4b). Fig. 4 compares the time profiles of the production of H<sub>2</sub>O<sub>2</sub> and 7-HC with bare TiO<sub>2</sub>, RuL<sub>3</sub>/TiO<sub>2</sub>, and curcumin/TiO<sub>2</sub> under visible light. The production of both H<sub>2</sub>O<sub>2</sub> and 7-HC in curcumin/TiO<sub>2</sub> was higher than that in bare TiO<sub>2</sub> and RuL<sub>3</sub>/TiO<sub>2</sub>, which is consistent with the previous results shown in Fig. 2 and 3. The generation of <sup>•</sup>OH in dye-TiO<sub>2</sub>

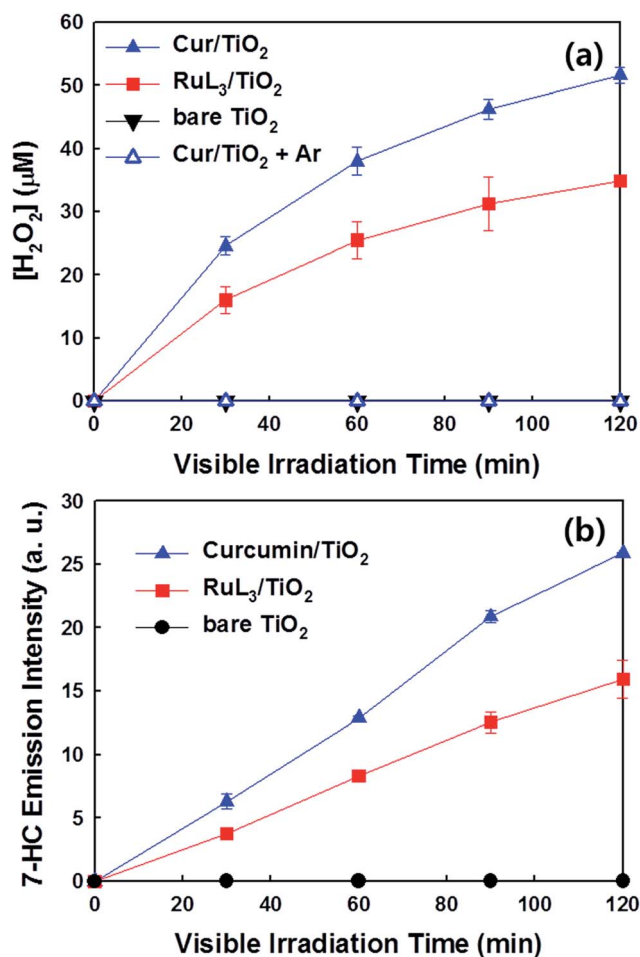


Fig. 4 Visible light-sensitized production of (a) H<sub>2</sub>O<sub>2</sub> through O<sub>2</sub> reduction and (b) 7-hydroxycoumarin (7-HC) as a coumarin-OH adduct (monitored by its photoluminescence) in the illuminated catalyst suspensions. The experimental conditions were [catalyst] = 0.5 g L<sup>-1</sup>, [EtOH]<sub>0</sub> = 10 mM (for a), [coumarin]<sub>0</sub> = 1 mM (for b), pH<sub>0</sub> = 3.0, λ > 420 nm, air-equilibrated for 30 min prior to irradiation except for the Ar-saturated case.

composite was further detected using EPR spin-trapping technique (Fig. 5). The peaks of DMPO-OH in the EPR spectra were confirmed in the dye-TiO<sub>2</sub> composite after visible light irradiation for 5 min, which ensure the formation of <sup>•</sup>OH *via* O<sub>2</sub> reduction.<sup>45</sup> In addition, the intensity of DMPO-OH peaks in curcumin/TiO<sub>2</sub> was higher than that in RuL<sub>3</sub>/TiO<sub>2</sub>. All results of the photo-activity tests confirmed the superior visible light activity of curcumin/TiO<sub>2</sub>.

Furthermore, the PEC properties of curcumin/TiO<sub>2</sub> and RuL<sub>3</sub>/TiO<sub>2</sub> electrodes were also compared. Fig. 6a shows the time profiles of photo-current generation using the electrodes of curcumin/TiO<sub>2</sub> and RuL<sub>3</sub>/TiO<sub>2</sub> under visible light irradiation. The photocurrent obtained with curcumin/TiO<sub>2</sub> is significantly higher than that obtained with RuL<sub>3</sub>/TiO<sub>2</sub>. Furthermore, we measured the electrochemical impedance spectrum (EIS) to investigate the charge-transfer efficiency under visible light irradiation. As shown in Fig. 6b, the radius of the semicircle in the EIS spectra decreased in the order of bare TiO<sub>2</sub> > RuL<sub>3</sub>/TiO<sub>2</sub>

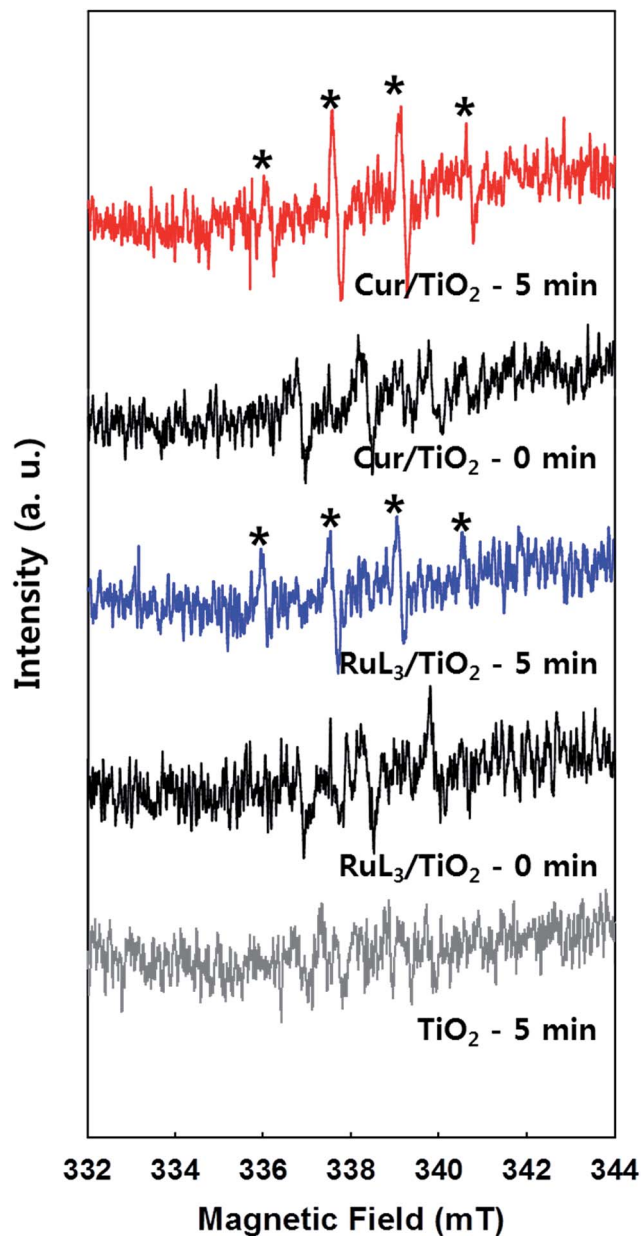


Fig. 5 EPR spectra of OH-DMPO (\*) adducts in the illuminated catalyst suspension. The experimental conditions were [catalyst] =  $1.5 \text{ g L}^{-1}$ , [DMPO]<sub>0</sub> = 90 mM, pH<sub>0</sub> = 3.0,  $\lambda > 420 \text{ nm}$ , air-equilibrated for 1 min prior to irradiation.

> curcumin/TiO<sub>2</sub>, which indicates that the interfacial charge-transfer resistance also decreased in the same order.<sup>46</sup> Both PEC results (Fig. 6a and b) indicate that the photo-induced electron transfer from the dye LUMO level to TiO<sub>2</sub> CB is more efficient in curcumin/TiO<sub>2</sub>. Thus, the enhanced photochemical activity of curcumin/TiO<sub>2</sub> is ascribed not only to enhanced visible light absorption, but also to more efficient interfacial charge transfer.

#### pH-Dependent activity under visible light irradiation

In the case of RuL<sub>3</sub>/TiO<sub>2</sub>, the negatively charged RuL<sub>3</sub> ( $\text{pK}_a < 3$ ) is anchored onto the positively charged TiO<sub>2</sub> surface through the

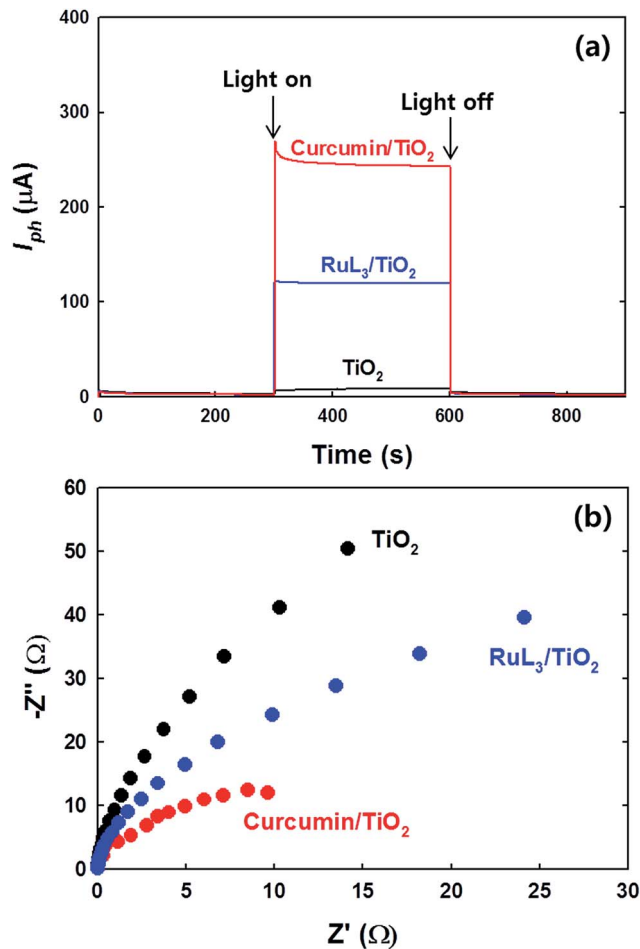


Fig. 6 (a) Photocurrent responses and (b) electrochemical impedance spectroscopic Nyquist plots of bare TiO<sub>2</sub>, RuL<sub>3</sub>/TiO<sub>2</sub>, and curcumin/TiO<sub>2</sub> electrodes under visible light. The experimental conditions were [NaClO<sub>4</sub>]<sub>0</sub> = 0.2 M, pH = 3.0, potential bias of +0.6 V (for a) and 0 V (for b) (vs. Ag/AgCl). The electrolyte solution was continuously N<sub>2</sub>-purged.

carboxylate group. This binding mechanism is sensitive to pH change since the surface charge of TiO<sub>2</sub> changes from positive to negative above pH 6 ( $\text{pH}_{\text{zpc}}$  of TiO<sub>2</sub>  $\approx 6$ ).<sup>37</sup> The negative surface charge on TiO<sub>2</sub> hinders the adsorption of the anionic RuL<sub>3</sub> sensitizer. This electrostatic repulsion between the sensitizer and TiO<sub>2</sub> surface is the primary reason for lower stability of RuL<sub>3</sub>/TiO<sub>2</sub> at pH > 6.<sup>18</sup> Fig. 7a shows that the adsorption of RuL<sub>3</sub> on TiO<sub>2</sub> steadily decreases from pH 3 to pH 9 while that of curcumin is much less affected by the pH change in the same condition, which indicates that the binding between curcumin and TiO<sub>2</sub> is only slightly affected by pH. Since curcumin is much less acidic than RuL<sub>3</sub> ( $\text{pK}_a \approx 8.89$ ),<sup>47</sup> the electrostatic repulsion between the negatively charged TiO<sub>2</sub> surface and the deprotonated curcumin should be significant only at pH > 9. As a result, the adsorption of curcumin is significantly higher than that of RuL<sub>3</sub> in the pH range of 3–9 (see Fig. 7a). Consequently, the photochemical and PEC activities of curcumin/TiO<sub>2</sub> are much less reduced when increasing pH from 3 to 9, whereas those of RuL<sub>3</sub>/TiO<sub>2</sub> decreased significantly when pH increased above 6 (Fig. 7b and c). The curcumin/TiO<sub>2</sub> that



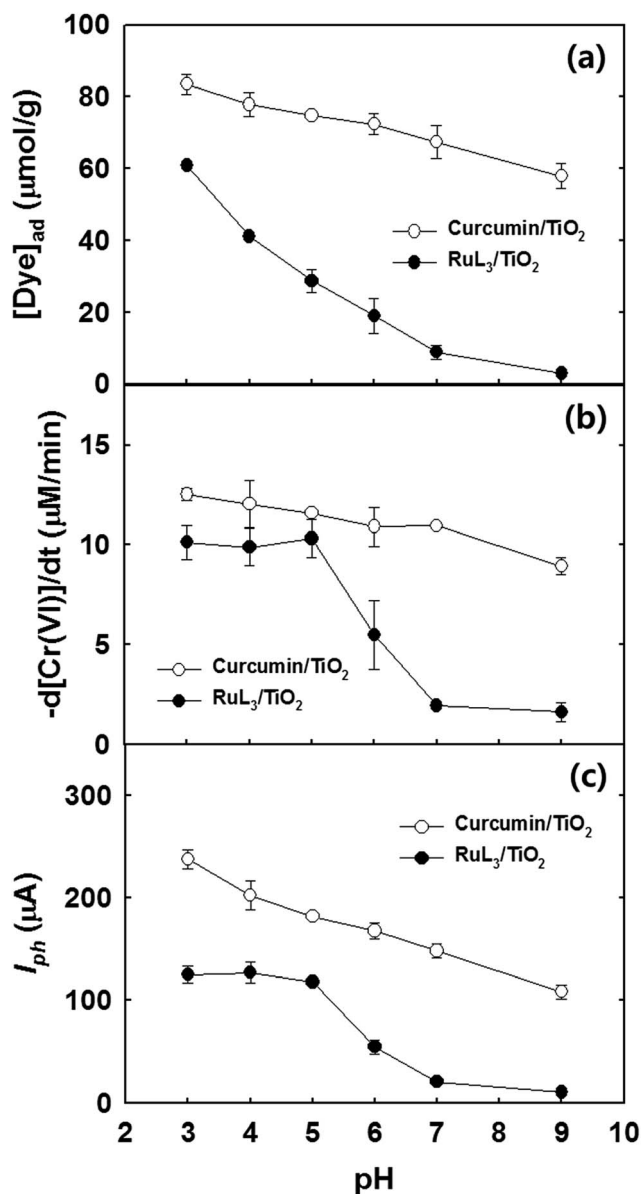


Fig. 7 pH-Dependent (a) adsorption isotherms of curcumin and RuL<sub>3</sub> in the aqueous suspension of TiO<sub>2</sub>, (b) visible light-sensitized removal of Cr(VI), and (c) photocurrent generation on curcumin/TiO<sub>2</sub> and RuL<sub>3</sub>/TiO<sub>2</sub> electrode. The experimental conditions were similar to those of Fig. 2 and 6.

employs an eco-friendly food dye as a sensitizer exhibits not only a higher photoactivity but also a higher stability in aquatic environment over a wide pH range.

The photostability of dye/TiO<sub>2</sub> was evaluated by repeating the cycles of DCA photodegradation using the same batch of catalyst (Fig. S4†). Each photodegradation cycle was carried out with using the dye/TiO<sub>2</sub> powder that was recovered from the previous cycle by filtering through 0.45 μm PTFE membrane, washing with distilled water, and the subsequent resuspension in a freshly prepared solution. Both curcumin and RuL<sub>3</sub> on TiO<sub>2</sub> exhibited serious deactivation during the repeated cycles of the photodegradation, which indicates that both dyes are degraded

on TiO<sub>2</sub> under visible light. Although the dye-sensitized TiO<sub>2</sub> system has been often referred as “photocatalytic” in the literature,<sup>48–50</sup> it is hardly “catalytic” in reality because of the instability of dye itself. The degradation of organometallic dyes may release metal ions into water, which makes their application to water purification unsuitable. On the other hand, natural and edible dyes like curcumin are acceptable as a visible light sensitizer for water treatment purpose although they might be degraded and released into water.

## Conclusions

The photochemical and PEC properties of curcumin-sensitized TiO<sub>2</sub> under visible light were investigated and compared with a well-known Ru-bipyridyl complex-sensitized TiO<sub>2</sub> system. The photochemical activities of curcumin/TiO<sub>2</sub> was much higher than those of RuL<sub>3</sub>/TiO<sub>2</sub> for the reduction of Cr(VI), the degradation of organic compounds, and the production of hydroxyl radicals and H<sub>2</sub>O<sub>2</sub> through O<sub>2</sub> reduction. As for the PEC properties, curcumin/TiO<sub>2</sub> electrode exhibited higher photocurrent generation and significantly lower charge transfer resistance compared to the RuL<sub>3</sub>/TiO<sub>2</sub> electrode system. More importantly, the adsorption of curcumin on the TiO<sub>2</sub> surface and the resulting photo-activity were consistently higher than those of RuL<sub>3</sub>/TiO<sub>2</sub> over a wide pH range. Therefore, the use of naturally-occurring, cheap and non-toxic curcumin as a sensitizer offers a practically viable method of TiO<sub>2</sub> activation under visible light for various solar environmental applications. However, it should be noted that the curcumin/TiO<sub>2</sub> like other dye-sensitized TiO<sub>2</sub> is not catalytic and stable at all and the dyes are degraded as a result of the sensitizing reactions in water. The curcumin dye should be considered as a sensitizing reagent which can be consumed as a result of photochemical reactions.

## Acknowledgements

This work was supported by Global Research Laboratory (GRL) Program (NRF-2014K1A1A2041044) and KCAP (Sogang Univ.) (2009–0093880), which were funded by the Korea Government (MSIP) through the National Research Foundation (NRF).

## References

- 1 H. Park, H.-i. Kim, G.-h. Moon and W. Choi, *Energy Environ. Sci.*, 2016, **9**, 8261–8272.
- 2 T. Tachikawa and T. Majima, *Chem. Soc. Rev.*, 2010, **39**, 4802–4819.
- 3 M. R. Hoffmann, S. T. Martin, W. Choi and D. W. Bahnemann, *Chem. Rev.*, 1995, **95**, 69–96.
- 4 Y. M. Huo, Z. F. Bian, X. Y. Zhang, Y. Jin, J. Zhu and H. X. Li, *J. Phys. Chem. C*, 2008, **112**, 6546.
- 5 G. Wu, T. Nishikawa, B. Ohtani and A. Chen, *Chem. Mater.*, 2007, **19**, 4530–4537.
- 6 J. Lim, D. Monllor-Satoca, J. S. Jang, S. Lee and W. Choi, *Appl. Catal., B*, 2014, **152–153**, 233–240.
- 7 J. B. Yin and X. P. Zhao, *Chem. Mater.*, 2004, **16**, 321–328.



- 8 H. Yu, X. J. Li, S. J. Zheng and W. Xu, *Mater. Chem. Phys.*, 2006, **97**, 59–63.
- 9 P. Wang, B. Huang, Y. Dai and M. H. Wangbo, *Phys. Chem. Chem. Phys.*, 2012, **14**, 9813–9825.
- 10 S. Linic, P. Christopher and D. B. Ingram, *Nat. Mater.*, 2011, **10**, 911–921.
- 11 A. Mikolajczyk, A. Malankowska, G. Nowaczyk, A. Gajewicz, S. Hirano, S. Jurga, A. Zaleska-Medynska and T. Puzyn, *Environ. Sci.: Nano*, 2016, **3**, 1425–1435.
- 12 H.-i. Kim, J. Kim, W. Kim and W. Choi, *J. Phys. Chem. C*, 2011, **115**, 9797–9805.
- 13 B. Liu, Y. Xue, J. Zhang, B. Han, J. Zhang, X. Suo, L. Mu and H. Shi, *Environ. Sci.: Nano*, 2017, **4**, 255–264.
- 14 J. Zhang, Y. Wang, J. Jin, J. Zhang, Z. Lin, F. Huang and J. Yu, *ACS Appl. Mater. Interfaces*, 2013, **5**, 10317–10324.
- 15 J. Yu, J. Zhang and M. Jaroniec, *Green Chem.*, 2010, **12**, 1611–1614.
- 16 G. Li, D. Zhang and J. C. Yu, *Environ. Sci. Technol.*, 2009, **43**, 7079–7085.
- 17 K. L. V. Joseph, J. Lim, A. Anthonysamy, H. Kim, W. Choi and J. K. Kim, *J. Mater. Chem. A*, 2015, **3**, 232–239.
- 18 Y. Park, S.-H. Lee, S. O. Kang and W. Choi, *Chem. Commun.*, 2010, **46**, 2477–2479.
- 19 Y. Park, W. Kim, D. Monllor-Satoca, T. Tachikawa, T. Majima and W. Choi, *J. Phys. Chem. Lett.*, 2013, **4**, 189–194.
- 20 J. Park, J. Yi, T. Tachikawa, T. Majima and W. Choi, *J. Phys. Chem. Lett.*, 2010, **1**, 1351–1355.
- 21 W. Kim, T. Tachikawa, T. Majima and W. Choi, *J. Phys. Chem. C*, 2009, **113**, 10603–10609.
- 22 A. Hagfeldt, G. Boschloo, L. Sun, L. Kloo and H. Pettersson, *Chem. Rev.*, 2010, **110**, 6595–6663.
- 23 E. Bae and W. Choi, *J. Phys. Chem. B*, 2006, **110**, 14792–14799.
- 24 H. Park, E. Bae, J.-J. Lee, J. Park and W. Choi, *J. Phys. Chem. B*, 2006, **110**, 8740–8749.
- 25 A. Mishra, M. K. R. Fischer and P. Bäuerle, *Angew. Chem., Int. Ed.*, 2009, **48**, 2474–2499.
- 26 Y. Wu, M. Marszalek, S. M. Zakeeruddin, Q. Zhang, H. Tian, M. Grätzel and W. Zhu, *Energy Environ. Sci.*, 2012, **5**, 8261–8272.
- 27 K. I. Priyadarsini, *J. Photochem. Photobiol., C*, 2009, **10**, 81–95.
- 28 B. B. Aggarwal, A. Kumar and A. C. Bharti, *Anticancer Res.*, 2003, **23**, 363–398.
- 29 R. A. Sharma, A. J. Gescher and W. P. Steward, *Eur. J. Cancer*, 2005, **41**, 1955–1968.
- 30 P. Anand, A. B. Kunnumakkara, R. A. Newman and B. B. Aggarwal, *Mol. Pharmaceutics*, 2007, **4**, 807–818.
- 31 H. Hatcher, R. Planalp, J. Cho, F. M. Torti and S. V. Torti, *Mol. Life Sci.*, 2008, **65**, 1631–1652.
- 32 N. Khan, F. Afaq and H. Mukhtar, *Antioxid. Redox Signaling*, 2008, **10**, 476.
- 33 T. Ganesh, J. H. Kim, S. J. Yoon, B. Kil, N. N. Maldar and J. W. Han, *Mater. Chem. Phys.*, 2010, **123**, 62–66.
- 34 *Standard Methods for the Examination of Water and Wastewater (20th ed.)*, ed. L. S. Clesceri, A. E. Greenberg and A. D. Eaton, American Public Health Association, Washington, DC, 1998.
- 35 H. Bader, V. Sturzenegger and J. Hoigne, *Water Res.*, 1988, **22**, 1109–1115.
- 36 J. Lim, P. Murugan, N. Lakshminarasimhan, J. Y. Kim, J. S. Lee, S.-H. Lee and W. Choi, *J. Catal.*, 2014, **310**, 91–99.
- 37 J. Kim, C. W. Lee and W. Choi, *Environ. Sci. Technol.*, 2010, **44**, 6849–6854.
- 38 S. Kundu and U. Nithiyanantham, *RSC Adv.*, 2013, **3**, 25278–25290.
- 39 B. Zebib, Z. Mouloungui and V. Noirot, *Bioinorg. Chem. Appl.*, 2010, **2010**, 1–8.
- 40 D. Yang, A. Velamakanni, G. Bozoklu, S. Park, M. Stoller, R. D. Piner, S. Stankovich, I. Jung, D. A. Field, C. A. Ventrone Jr and R. S. Ruoff, *Carbon*, 2009, **47**, 145–152.
- 41 R. He, X. Hu, H. C. Tan, J. Feng, C. Steffi, K. Wang and W. Wang, *J. Mater. Chem. B*, 2015, **3**, 2137–2146.
- 42 S. Kim and W. Choi, *Environ. Sci. Technol.*, 2002, **36**, 2019–2025.
- 43 S. Kim, S.-J. Hwang and W. Choi, *J. Phys. Chem. B*, 2005, **109**, 24260–24267.
- 44 H. Park, Y. Park, W. Kim and W. Choi, *J. Photochem. Photobiol., C*, 2013, **15**, 1–20.
- 45 J. Lim, H. Kim, P. J. J. Alvarez, J. Lee and W. Choi, *Environ. Sci. Technol.*, 2016, **50**, 10545–10553.
- 46 N. Lakshminarasimhan, A. D. Bokare and W. Choi, *J. Phys. Chem. C*, 2012, **116**, 17531–17539.
- 47 Z. Wang, M. H. M. Leung, T. W. Kee and D. S. English, *Langmuir*, 2009, **26**, 5520–5526.
- 48 P. Chowdhury, J. Moreira, H. Gomaa and A. K. Ray, *Ind. Eng. Chem. Res.*, 2012, **51**, 4523–4532.
- 49 J. Moon, C. Y. Yun, K.-W. Chung, M.-S. Kang and J. Yi, *Catal. Today*, 2003, **87**, 77–86.
- 50 M. S. Dieckmann and K. A. Gray, *Water Res.*, 1996, **30**, 1169–1183.
- 51 A. Dayton, K. Selvendiran, M. L. Kuppusamy, B. K. Rivera, S. Meduru, T. Kálai, K. Hideg and P. Kuppusamy, *Cancer Biol. Ther.*, 2010, **10**, 1027–1032.
- 52 U. Singh, S. Verma, H. N. Ghosh, M. C. Rath, K. I. Priyadarsini, A. Sharma, K. K. Pushpa, S. K. Sarkar and T. Mukherjee, *J. Mol. Catal. A: Chem.*, 2010, **318**, 106–111.

